Progress In Electromagnetics Research C, Vol. 172, 286–300, 2026

PIER C

(Received 15 June 026, Accepted 17 July 2026, Scheduled 12 August 2026)

Comparative Performance Evaluation of OOK, DPSK, and Optical OFDM in an EDFA-Assisted 8-Channel WDM-FSO System

Tejas Patel*, Shailesh Khant, and Atul Patel

Faculty of Computer Science and Applications (CMPICA), Charotar University of Science and Technology (CHARUSAT)
Anand, Gujarat, India

ABSTRACT: Free Space Optical (FSO) communication is a high-capacity optical wireless technology for terrestrial backhaul, interbuilding connectivity, and rapidly deployable networks, but fog attenuation, turbulence, and beam-divergence-induced spreading degrade link reliability. This paper evaluates an impairment-aware erbium-doped fiber amplifier (EDFA)-assisted 8-channel, wavelength division multiplexing free-space optical (WDM-FSO) system using On-Off Keying (OOK), Differential Phase Shift Keying (DPSK), and Optical Orthogonal Frequency Division Multiplexing (Optical OFDM). The system uses eight C-band wavelengths from 1552 nm to 1566 nm with 2 nm spacing, each carrying 10 Gbps, and employs a fixed 20 dB EDFA gain for attenuation compensation. Beer-Lambert propagation loss, Kim visibility-based fog model, log-normal and Gamma-Gamma turbulence models, beam-divergence-induced geometric spreading, WDM filter isolation, laser launch-power fluctuation, and receiver-side DSP-assisted normalization are considered. RSoft OptSim simulations are performed over 1–8 km link distances and 50–500 m visibility. Performance is evaluated using bit error rate (BER), Q-factor, and signal-to-noise ratio (SNR). Under the specified simulation assumptions, Optical OFDM achieves the best performance among the compared schemes, with 1.0×10^{-9} BER at 10 Gbps and 1.2×10^{-6} BER, 4.72 Q-factor, and 17.0 dB SNR at 8 km.

1. INTRODUCTION

Free Space Optical (FSO) communication has gained significant attention as a high-capacity optical wireless technology for terrestrial backhaul, inter-building connectivity, disaster recovery networks, and rapidly deployable communication links [1, 2]. It offers several advantages, including large bandwidth, license-free spectrum, low installation cost, high data rate transmission, and immunity to electromagnetic interference [1, 2]. Due to these benefits, FSO is considered a strong alternative or complementary solution to conventional radio-frequency and fiber-based communication systems. However, the practical deployment of FSO links is strongly limited by atmospheric channel conditions [1–3]. Fog, haze, rain, atmospheric attenuation, and turbulence-induced irradiance fluctuations reduce received optical power, increase bit error rate (BER), and degrade overall link reliability [2–5]. Among these impairments, fog is one of the most critical because its scattering effect can severely attenuate the optical signal and reduce the achievable transmission distance [3, 5, 6].

Figure 1 shows the proposed N-channel WDM-FSO system with an EDFA. Multiple laser sources are combined using a WDM multiplexer, amplified by an EDFA booster, and transmitted through the FSO channel using a Tx telescope. The FSO channel includes atmospheric effects, such as haze, fog, rain, and turbulence. At the receiver side, the signal is collected by the Rx telescope, amplified by an EDFA pre-amplifier, separated using a WDM demultiplexer, and detected by photodetectors. This setup is used to analyze WDM-FSO performance under different atmospheric conditions [7–9].

To improve capacity and reliability of FSO systems, several techniques have been investigated, including Wavelength Division Multiplexing Free Space Optical (WDM-FSO) transmission, optical amplification, atmospheric channel modeling, and advanced modulation schemes [7, 9–11]. WDM-FSO increases system capacity by transmitting multiple optical wavelengths through the same free-space channel [7–9, 12]. Erbium-Doped Fiber Amplifier (EDFA) is commonly used to compensate for optical power loss and improve receiver sensitivity [7, 10, 13]. In addition, modulation techniques such as On-Off Keying (OOK), Differential Phase Shift Keying (DPSK), and Optical Orthogonal Frequency Division Multiplexing (Optical OFDM) have been studied to enhance transmission performance under atmospheric impairments [11, 14–16].

Although existing studies have contributed significantly to FSO system analysis, many of them focus on single-channel links, limited atmospheric conditions, or individual modulation techniques [11, 14, 15, 17]. Comprehensive evaluation of multi-channel WDM-FSO systems under visibility-dependent fog attenuation and turbulence-induced fading remains comparatively limited [3, 6, 18–20]. Moreover, few studies jointly compare OOK, DPSK, and Optical OFDM within the same EDFA-assisted WDM-FSO framework using BER, Q-factor, and SNR as common performance metrics [10, 14–16]. This creates a need for a unified model that can provide a more realistic performance assessment under fog-prone terrestrial environments.

* Corresponding author: Tejas Patel (tejaspatel.mca@charusat.ac.in).

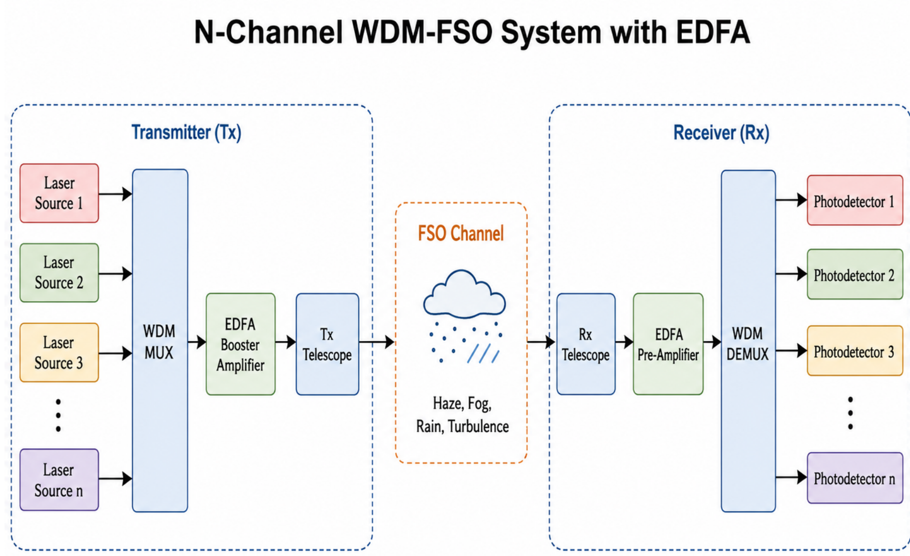

FIGURE 1. N-channel WDM-FSO system with EDFA.

To address this gap, this paper proposes an atmospheric impairment-aware 8-channel WDM-FSO system with EDFA operating in the optical C-band. The system uses eight wavelengths from 1552 nm to 1566 nm with 2 nm channel spacing, where each channel carries 10 Gbps data. A 20 dB EDFA is incorporated to compensate atmospheric attenuation loss and improve received signal quality. The atmospheric channel is modeled using Beer-Lambert propagation loss and the Kim visibility-based attenuation model, while log-normal and Gamma-Gamma distributions are used to represent weak and strong turbulence conditions [3, 4, 11, 14]. The complete system is simulated in RSoft OptSim over 1–8 km link distances and 50–500 m fog-impaired visibility conditions.

The main contributions of this work are as follows. First, an EDFA-assisted 8-channel C-band WDM-FSO system is evaluated for high-capacity optical wireless transmission under a unified impairment-aware simulation framework. Second, visibility-dependent fog attenuation, Beer-Lambert propagation loss, turbulence-aware channel modeling, and beam-divergence-induced geometric spreading are integrated into the system model. Third, OOK, DPSK, and Optical OFDM are compared under the same link configuration, wavelength allocation, EDFA gain, receiver condition, and performance metrics. Fourth, this study clarifies the OFDM configuration, simulated and analytical BER evaluation procedure, EDFA noise contribution, WDM filter isolation, laser launch-power fluctuation, and receiver-side DSP-assisted normalization, and further evaluates these practical impairments through a compact sensitivity analysis. These additions are motivated by prior studies on fog-impaired FSO channels, turbulence-aware optical wireless links, WDM-FSO systems, and modulation-dependent FSO performance evaluation [11, 14–16]. Therefore, the practical significance of the work lies in identifying the modulation behavior of an EDFA-assisted WDM-FSO link when both atmospheric and system-level impairments are considered.

The aim of this study is to evaluate the reliability of an EDFA-assisted 8-channel WDM-FSO system under adverse atmospheric conditions and to determine the modulation scheme that provides the best performance under specified simulation assumptions. The rest of the paper is organized as follows. Section 2 reviews related work on atmospheric impairment-aware FSO and WDM-FSO systems. Section 3 describes the proposed system model, fair-comparison setup, channel modeling, EDFA and WDM assumptions, OFDM configuration, and receiver-side DSP processing. Section 4 presents the simulation results and practical impairment sensitivity analysis. Section 5 discusses the observed performance trends, OFDM advantages, and practical limitations. Section 6 concludes the paper with key findings and future research directions.

2. RELATED WORK

Recent studies on WDM-FSO systems show that atmospheric attenuation and turbulence strongly affect link reliability, receiver sensitivity, and BER performance. Fog is considered the most critical impairment because scattering and absorption greatly reduce optical signal strength.

From the reviewed literature, it is observed that most existing studies focus on high-capacity DWDM/MDM-FSO systems, EDFA-based loss compensation, atmospheric modeling, or individual modulation techniques. However, limited work jointly considers an 8-channel C-band WDM-FSO system with EDFA, visibility-dependent fog attenuation, turbulence-aware channel modeling, and comparative performance analysis of OOK, DPSK, and Optical OFDM using BER, Q-factor, and SNR. Therefore, the present work addresses this gap by developing a unified simulation framework for evaluating reliable high-capacity WDM-FSO transmission under fog-impaired and turbulence-affected atmospheric conditions. Table 1 summarizes representative recent studies on atmospheric impairment-aware FSO systems and highlights the corresponding research gaps addressed in this work.

TABLE 1. Summary of recent research on atmospheric impairment-aware FSO systems.

Ref. No.	Key Findings	Research Gap
[19]	Shows that DWDM-FSO can support high-capacity transmission, but adverse weather strongly affects link quality and BER.	Does not focus on 8-channel C-band WDM-FSO with EDFA and comparative OOK, DPSK, and Optical OFDM analysis.
[13]	Demonstrates that EDFA-based loss compensation improves received signal strength and supports high-speed FSO transmission.	Limited emphasis on visibility-dependent fog modeling and multi-modulation comparison in WDM-FSO links.
[2]	Reviews major FSO challenges such as turbulence, weather loss, alignment, hybrid links, modulation, and coding.	Being a survey, it does not provide a dedicated simulation framework for EDFA-assisted WDM-FSO under fog and turbulence.
[3]	Presents atmospheric modeling approaches for FSO links under realistic propagation conditions.	Does not evaluate WDM channel allocation, EDFA gain, and modulation performance together.
[5]	Discusses improvement of FSO performance under weather-related impairments.	Limited comparison of OOK, DPSK, and Optical OFDM in a unified 8-channel WDM-FSO system.
[11]	Summarizes channel models and modulation methods used to improve FSO link performance.	Does not provide new system-level results for fog-resilient WDM-FSO with EDFA.
[20]	Shows that MDM-WDM can increase capacity and DP-QPSK can improve performance under fog conditions.	Focuses on DP-QPSK and MDM-WDM rather than OOK, DPSK, and Optical OFDM comparison.
[6]	Evaluates MDM-WDM FSO performance under realistic weather conditions.	Does not consider EDFA-assisted 8-channel WDM-FSO with visibility-dependent fog attenuation and OFDM comparison.
[17]	Shows the suitability of FSO links for 5G services under different geographical and weather conditions.	Does not deeply compare multiple modulation schemes within an EDFA-assisted WDM-FSO architecture.
[21]	Demonstrates that programmable optical processing can help reduce turbulence-induced degradation.	Focuses on turbulence-mitigation hardware rather than WDM-FSO modulation and EDFA-based system evaluation.
[12]	Shows that WDM-FSO can enhance capacity and support 5G mobility applications.	Does not jointly analyze fog attenuation, turbulence, EDFA, and OOK/DPSK/Optical OFDM performance.
[16]	Compares modulation schemes in a hybrid MDM-OFDM RoFSO system.	Focus is on RoFSO/MDM-OFDM, not conventional 8-channel WDM-FSO with EDFA under fog visibility conditions.
[22]	Shows that wavelength diversity can improve outage probability and BER performance.	Does not include EDFA compensation or detailed comparison of OOK, DPSK, and Optical OFDM.
[23]	Demonstrates improved long-range FSO performance using advanced modulation and coding.	Does not address WDM-FSO operation under visibility-dependent fog and turbulence.
[24]	Shows that dust conditions affect data rate and FSO link performance.	Focuses on dust impairment rather than fog, turbulence, EDFA, and WDM-based multi-channel transmission.
[25]	Proposes multi-hop FSO-UWOC communication for reliable inter-island links.	Application is hybrid FSO-UWOC, not terrestrial WDM-FSO with EDFA and modulation comparison.

Recent studies from [26–37] further highlight the rapid development of high-capacity FSO systems for 5G, smart city, and long-range optical wireless applications. Kumar and Krishnan [26, 27] investigated RoFSO links with spatial diversity and showed that diversity techniques improve link reliability under combined channel impairments. Singh et al. [28], Dutta et al. [29], and Singh et al. [30] explored high-speed FSO transmission using orbital angular momentum and WDM/OAM multiplexing, demonstrating that advanced multiplexing can significantly enhance channel capacity. Singh and Malhotra [31] compared modulation schemes in MDM radio-over-FSO links and confirmed that modulation selection strongly affects BER and link stability under turbulence. El-Qady and Abaza [32] studied multi-hop relay-based FSO systems and showed that relay-assisted transmission improves performance under atmospheric turbulence. Qu et al. [33] proposed a wavelength-shift-keying-based bidirectional FSO link for last-mile access, while Singh et al. [34] demonstrated high-capacity PAM-4-based hybrid PDM-OAM FSO transmission. Wen et al. [35] investigated DCO-OFDM-based FSO-integrated sensing and communication, showing the suitability of OFDM for advanced optical wireless systems. Aljohani et al. [36] introduced a regeneration technique to improve FSO signal quality, and Bekkali et al. [37] presented an optical beam stabilizer for next-generation FSO systems. Overall, these works confirm that multiplexing, diversity, relay, OFDM, regeneration, and beam stabilization techniques can improve FSO performance; however, limited attention is given to EDFA-assisted 8-channel WDM-FSO systems under visibility-dependent fog attenuation with comparative OOK, DPSK, and Optical OFDM analyses.

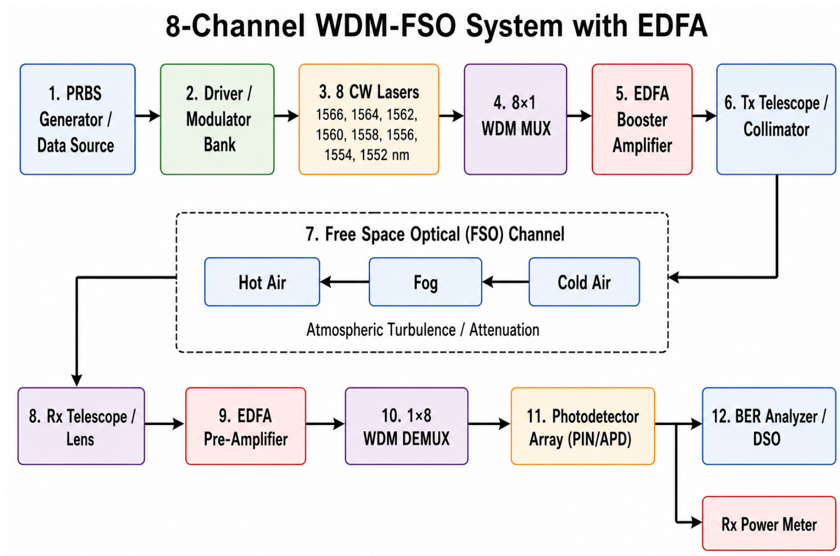

FIGURE 2. Proposed EDFA-assisted 8-channel WDM-FSO system.

From the reviewed literature, it can be observed that existing FSO and WDM-FSO studies have individually considered atmospheric attenuation, turbulence, EDFA-assisted transmission, modulation-format comparison, or real-weather operation [3, 6, 10, 13, 17]. However, the joint consideration of fair modulation comparison, explicit OFDM configuration, EDFA noise contribution, WDM filter isolation, beam-divergence-induced geometric loss, laser launch-power fluctuation, and receiver-side DSP-assisted mitigation remains limited. This gap motivates the impairment-aware evaluation framework adopted in this work.

3. METHODOLOGY

3.1. System Architecture

This work presents the design and performance evaluation of an eight-channel Wavelength Division Multiplexing Free Space Optical (WDM-FSO) communication system operating under fog-impaired atmospheric conditions. In contrast to conventional comparative modulation studies, the proposed work integrates atmospheric attenuation modeling, turbulence-induced fading analysis, and modulation-dependent BER, Q-factor, and SNR evaluation within a multi-channel optical wireless framework. The system investigates the transmission behavior of OOK, DPSK, and Optical OFDM modulation schemes under visibility degradation and long-distance propagation.

For clarity, Fig. 2 should be interpreted with a left-to-right signal-flow direction from the transmitter section to the receiver section. The EDFA before the FSO channel acts as a booster amplifier, while the EDFA after the FSO channel acts as a receiver-side pre-amplifier.

Figure 2 shows the proposed 8-channel WDM-FSO system with an EDFA in a simplified block diagram. Eight C-band laser channels from 1566 nm to 1552 nm are modulated, combined using an 8×1 WDM multiplexer, amplified by an EDFA booster, and transmitted through the FSO atmospheric channel. At the receiver side, the signal is collected, amplified by an EDFA pre-amplifier, separated using a 1×8 WDM demultiplexer, and detected by a PIN/APD photodetector array. The BER analyzer, DSO, and power meter are used to evaluate BER, Q-factor, SNR, and received power. The detailed transmitter and receiver simulation blocks are shown in Figs. 3 and 4.

The WDM demultiplexer is considered as a practical non-ideal optical filter bank rather than an ideal channel separator. Therefore, adjacent-channel leakage and possible channel-power imbalance are considered important WDM-related impairments. In the baseline comparison, the WDM demultiplexer is assumed to provide at least 30 dB channel isolation across the 1552–1566 nm wavelength range, while reduced isolation values of 20 dB and 15 dB are considered as sensitivity cases for evaluating imperfect WDM filtering. Under lower isolation conditions, increased inter-channel leakage degrades the detected signal quality. This clarification separates WDM-filter-related penalties from modulation-dependent performance differences.

As shown in Fig. 3, the system uses the optical C-band, and the eight wavelengths range from 1566 nm to 1552 nm. Each optical channel is generated using a continuous-wave laser source and independently modulated using OOK, DPSK, or Optical OFDM schemes to evaluate modulation-dependent BER, Q-factor, SNR, transmission robustness, and noise resilience under fog-impaired atmospheric conditions. The channels are multiplexed using a WDM multiplexer and transmitted through the FSO channel. The simulation is performed using the RSoft OptSim platform.

To include source-level practical impairment, laser output fluctuation is modeled as a relative variation around the nominal launch power. The instantaneous transmitted optical power is represented as

$$P_t(t) = P_{t,0}[1 + \delta_p(t)] \tag{1}$$

where $P_{t,0}$ is the nominal transmitted optical power, and $\delta_p(t)$ represents the relative laser power fluctuation. In the baseline

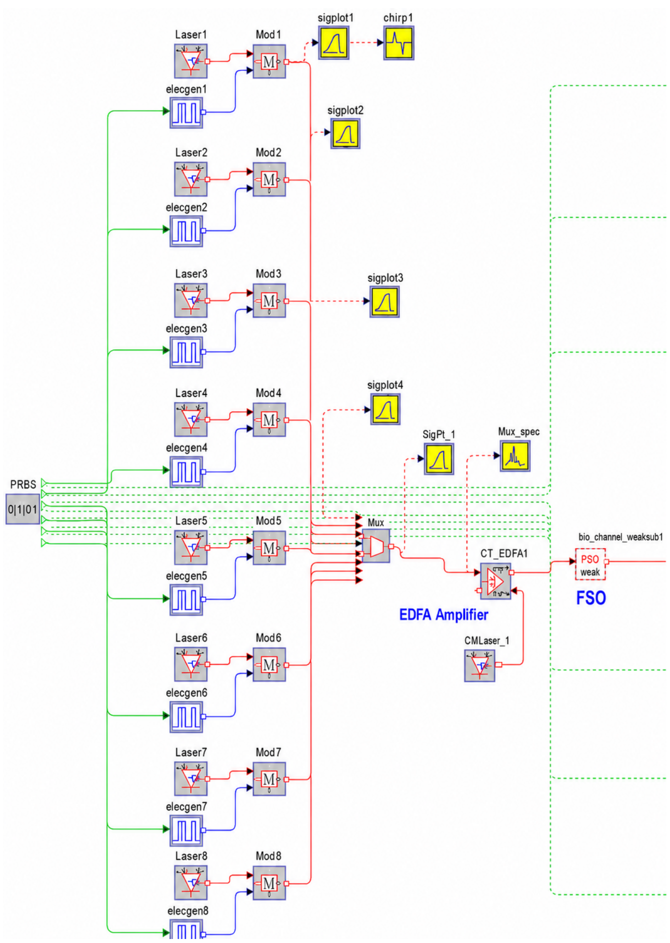

FIGURE 3. Transmitter-side implementation of the 8-channel WDM-FSO system showing parallel laser/modulator branches, WDM multiplexing, EDFA amplification, and FSO-channel input.

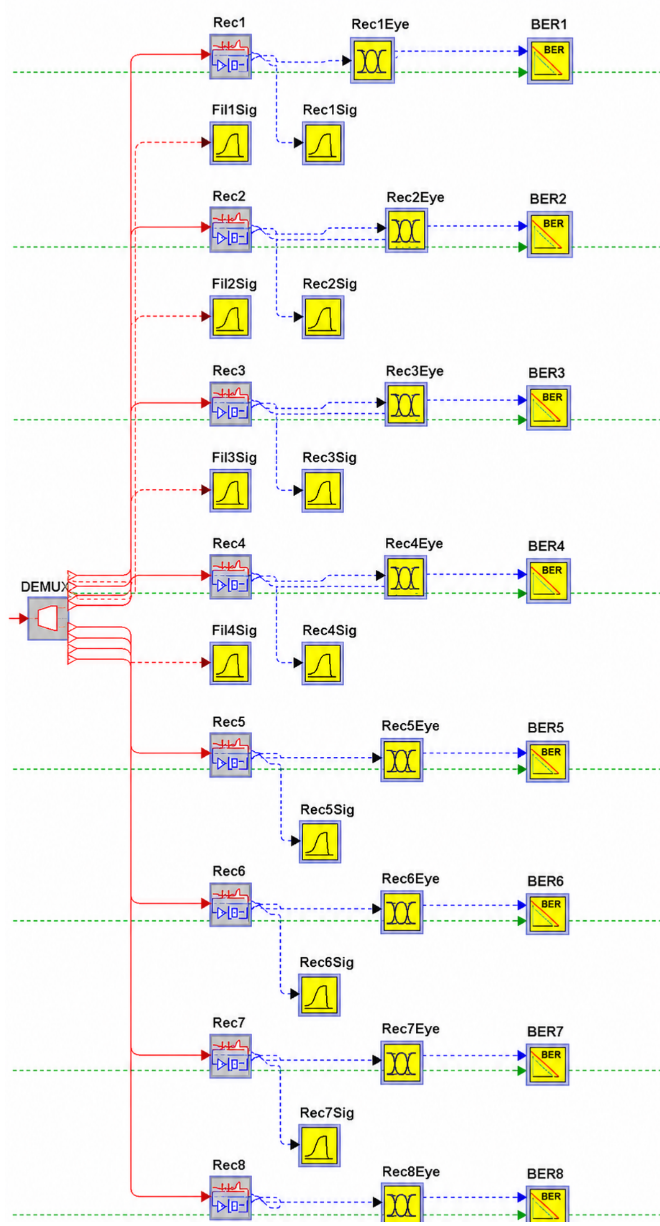

FIGURE 4. Receiver-side implementation showing 1×8 WDM demultiplexing, photodetection, eye-diagram monitoring, filtering, and BER analysis for each WDM channel.

comparison, the same nominal launch-power range is maintained for all modulation formats. The laser fluctuation effect is treated as a sensitivity condition in this analysis to evaluate how small source-power variations influence received power, BER, Q-factor, and SNR.

Figure 4 shows the receiver section, where the signals are demultiplexed, detected, and analyzed. To emulate realistic atmospheric propagation conditions, visibility-dependent fog attenuation is varied from 20 dB/km to 100 dB/km across transmission distances ranging from 1 km to 8 km. This enables the investigation of modulation robustness under fog-impaired environments encountered in practical terrestrial FSO deployments. Turbulence is also simulated using log-normal and Gamma-Gamma distributions for weak and strong turbulence, respectively. The Beer-Lambert law is used to simulate signal attenuation. Performance is evaluated using BER, Q-factor, and SNR.

The combined fog attenuation and turbulence framework enables a more realistic characterization of WDM-FSO channel impairments than conventional attenuation-only simulation models. The novelty of this work lies in the comprehensive performance comparison of different modulation schemes in a multi-channel WDM-FSO system with fog and turbulence effects.

3.2. Free Space Optical Channel Model

The optical signal propagates through a free-space channel affected by atmospheric attenuation and turbulence. The received optical power considering geometric spreading, atmospheric attenuation, and turbulence-induced fading is modeled as

$$P_r = P_t \cdot H_{geo} \cdot H_{atm} \cdot H_{turb} \tag{2}$$

where H_{geo} represents geometric losses; H_{atm} represents the atmospheric attenuation; and H_{turb} represents the turbulence-induced fading.

In addition to atmospheric attenuation and turbulence, beam divergence is included via the geometric spreading factor H_{geo}. For a transmitter aperture diameter D_t, receiver aperture diameter D_r, beam divergence angle θ, and propagation distance L, the geometric coupling term is approximated as:

$$H_{geo} = \left(\frac{D_r}{D_t + \theta L}\right)^2 \quad (3)$$

This expression shows that a larger divergence angle increases beam spreading over long distances and reduces the fraction of optical power collected by the receiver aperture. Therefore, beam divergence directly affects the received optical power, BER, Q-factor, and SNR, especially at longer FSO link distances.

3.3. Fog Attenuation Model

Fog is considered the most severe atmospheric impairment in terrestrial FSO systems due to strong Mie scattering produced by suspended water droplets, resulting in significant optical power degradation and reduced transmission reliability. Atmospheric attenuation can be expressed using the Beer-Lambert law:

$$P_r = P_t e^{-\gamma L} \quad (4)$$

where P_r is the received power; P_t is the transmitted power; γ is the attenuation coefficient (dB/km); and L is the propagation distance.

The attenuation coefficient is calculated using the Kim visibility model as:

$$\gamma = \frac{3.91}{V}\left(\frac{\lambda}{550}\right)^{-q} \quad (5)$$

where V is the visibility (km); λ is the wavelength (nm); and q is the particle size distribution coefficient. For dense fog, $q = 0$.

The Kim atmospheric attenuation model is selected because of its suitability for dense fog environments and wavelength-dependent attenuation estimation in optical wireless communication systems operating within the C-band spectrum.

3.4. Turbulence Model

Atmospheric turbulence causes random irradiance fluctuations known as scintillation. For weak turbulence conditions, the log-normal distribution can be used:

$$I = I_0 e^X \quad (6)$$

where X is a Gaussian random variable.

Under dense fog conditions, random refractive index fluctuations introduce strong irradiance scintillation effects, which significantly degrade signal stability and receiver sensitivity. Therefore, the log-normal and Gamma-Gamma turbulence models are used. The probability density function is expressed as

$$p(I) = \frac{2(\alpha\beta)^{\frac{\alpha+\beta}{2}}}{\Gamma(\alpha)\Gamma(\beta)} I^{\frac{\alpha+\beta}{2}-1} K_{\alpha-\beta}\left(2\sqrt{\alpha\beta I}\right), \quad I > 0 \quad (7)$$

where α represents large-scale turbulence effects; β represents small-scale turbulence effects; and K is the modified Bessel function.

An erbium-doped fiber amplifier (EDFA) is incorporated to compensate atmospheric propagation losses and improve receiver sensitivity under high-attenuation fog conditions. In the system model, the EDFA is not treated only as an ideal gain block; its practical noise contribution is represented through the amplifier noise figure and amplified spontaneous emission noise contribution included in the receiver-noise-limited performance evaluation. A fixed EDFA gain of 20 dB is used for all modulation formats to maintain a fair comparison. The EDFA is assumed to provide nearly flat gain across the eight C-band WDM channels, and possible residual gain imbalance is considered as a practical limitation of the WDM-FSO link rather than a modulation-dependent effect.

3.5. Receiver Model

The received signal is de-multiplexed and detected. For OOK, direct detection is used. The decision threshold is

$$I_{th} = \frac{I_1 + I_0}{2} \quad (8)$$

For DPSK, differential detection is applied by comparing the phase difference between consecutive symbols. For Optical OFDM, Fast Fourier Transform processing is employed to recover orthogonal subcarriers and improve receiver-side subcarrier recovery and robustness against atmospheric-induced signal degradation.

To mitigate beam-divergence-induced received-power reduction at longer link distances, a receiver-side DSP-assisted normalization and threshold-adjustment stage is included after photodetection and electrical filtering. The DSP stage estimates the average received signal level for each WDM channel and applies channel-wise amplitude normalization before decision thresholding. For an electrical received sample r_i, the normalized sample is expressed as

$$\hat{r}_i = \frac{r_i}{\mu_r + \epsilon} \quad (9)$$

where μ_r is the estimated mean received signal level over the observation window, and ϵ is a small constant used to avoid numerical instability. The decision threshold is then adjusted according to the normalized signal level. This DSP step does not compensate atmospheric attenuation itself, but it reduces the decision-level mismatch caused by beam spreading, channel-power imbalance, and received-power fluctuations.

The performance of the WDM-FSO system is evaluated using the bit error rate, Q-factor, and signal-to-noise ratio. The receiver output quality is first evaluated using the Q-factor, which represents receiver signal integrity and decision reliability. The Q-factor corresponding to a given BER can be expressed as:

$$Q = \sqrt{2} \cdot \text{erfc}^{-1}(2 \cdot \text{BER}) \quad (10)$$

where Q is the quality factor; $\text{erfc}^{-1}(\cdot)$ is the inverse complementary error function; and BER is the bit error rate.

For a Gaussian-noise-limited optical receiver, the BER corresponding to a given Q-factor can be approximated as:

$$\text{BER} = \frac{1}{2}\text{erfc}\left(\frac{Q}{\sqrt{2}}\right) \quad (11)$$

TABLE 2. Simulation parameters for 8-Channel WDM-FSO system.

Parameter	Value
Number of WDM channels	8
Wavelengths (nm)	1566, 1564, 1562, 1560, 1558, 1556, 1554, 1552
Channel spacing	2 nm
WDM demultiplexer filter isolation	Baseline $\geq$ 30 dB; sensitivity cases at 20 dB and 15 dB
WDM crosstalk consideration	Adjacent-channel leakage and channel-power imbalance considered as practical WDM impairments
Modulation schemes	OOK, DPSK, Optical OFDM
Optical transmitter	Continuous wave laser
Laser fluctuation model	Relative launch-power fluctuation, $P_t(t) = P_{t,0}[1 + \delta_p(t)]$
Laser fluctuation range for sensitivity analysis	$\pm 1\%$ to $\pm 3\%$ around nominal launch power
Transmit power	0–10 dBm
Link distance	1–8 km
Beam divergence	1–2 mrad; included in geometric spreading loss H_{geo}
Transmitter aperture diameter	5–10 cm
Receiver aperture diameter	20–30 cm
Optical amplifier	EDFA
EDFA gain	20 dB
EDFA noise figure	5 dB
EDFA gain flatness assumption	Flat gain across 1552–1566 nm WDM channels
Turbulence model	Log-normal and Gamma-Gamma turbulence models
Atmospheric condition	Fog
Visibility range	50–500 m
Attenuation coefficient	20–100 dB/km, visibility-dependent fog attenuation range used in the simulation
Receiver-side DSP stage	Channel-wise amplitude normalization and adaptive decision-threshold adjustment
Performance evaluation metrics	BER, Q-factor, SNR

Equations (7) and (8) are inverse forms of the same Q-factor-BER relationship. Therefore, Eq. (7) is used to relate the receiver-quality metric to BER, while Eq. (8) is used to calculate the analytical BER reference reported in Tables 4–6.

The electrical Signal-to-Noise Ratio considering attenuation-induced received power reduction and receiver noise contributions is calculated as:

$$\text{SNR} = \frac{(R \cdot P_t e^{-\gamma L})^2}{2qRP_t e^{-\gamma L} B + \frac{4kTB}{R_L}} \tag{12}$$

where R is the photodetector responsivity; P_t is the transmitted power; γ is the attenuation coefficient; L is the link distance; q is the electron charge; k is the Boltzmann constant; T is the temperature; B is the bandwidth; and R_L is the load resistance.

3.6. Fair Comparison and BER Evaluation Method

For a fair comparison of OOK, DPSK, and Optical OFDM, the same 8-channel WDM-FSO link configuration is maintained for all modulation schemes. The wavelength set, channel spacing, link distance, visibility range, fog attenuation model, turbulence model, EDFA gain, receiver aperture, and performance metrics are kept identical. The average optical launch-power range is also kept the same for all modulation formats. For fixed-distance and visibility-based evaluations, the nominal per-channel data rate is maintained at 10 Gbps, while in the bit-rate sweep, the same bit-rate values are applied to all three modulation schemes.

In the BER-related result tables, the term "simulated BER" denotes the BER obtained from the RSoft OptSim receiver/BER-analyzer output for each simulated link condition. The term "analytical BER" denotes the BER calculated using the analytical Q-factor and receiver-noise relationship given in Eq. (8) together with the received-power and SNR formulation in Eq. (9). The BER vs bit-rate and BER vs distance tables report both simulated and analytical BER values, while the visibility-dependent BER table is reported as a simulated BER analysis. Thus, the simulated values represent system-level simulation results, whereas the analytical values provide a theoretical reference for validating observed BER trends where applicable.

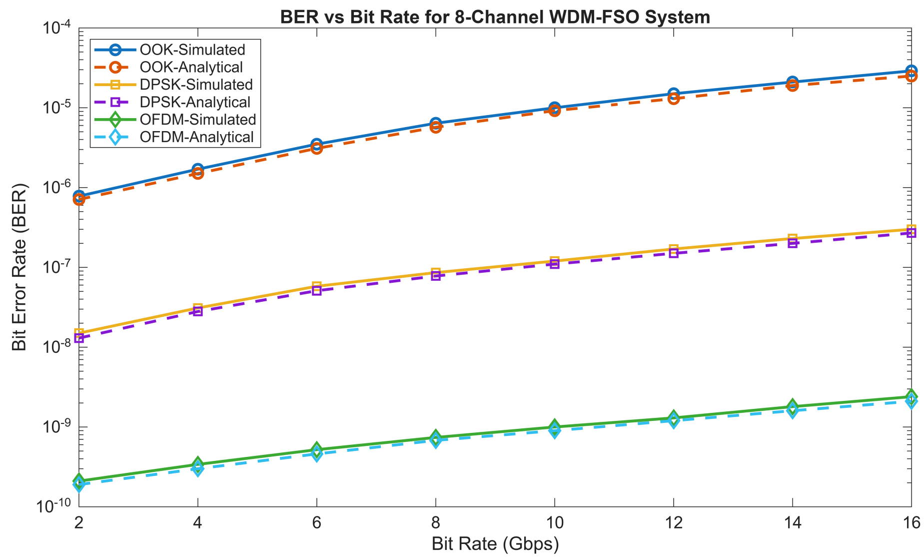

FIGURE 5. BER vs bitrate.

TABLE 3. Optical OFDM configuration used in the simulation.

Parameter	Value
OFDM type	DCO-OFDM for IM/DD optical transmission
FFT size	128
Number of active data subcarriers	52
Number of pilot subcarriers	4
Cyclic prefix length	16 samples, corresponding to $1/8$ of the FFT size
Subcarrier modulation	QPSK
Per-channel gross data rate	Nominal 10 Gbps; varied according to the bit-rate sweep for BER vs bit-rate analysis
Receiver processing	Cyclic-prefix removal, FFT-based subcarrier recovery, pilot-aided phase correction, and BER evaluation

To make the Optical OFDM configuration explicit and reproducible, the OFDM transmitter and receiver parameters used in the simulation setup are summarized in Table 3. These parameters define the fixed OFDM setup used to obtain the OFDM performance results reported in the BER, Q-factor, and SNR analyses. The same OFDM configuration is maintained for the distance, visibility, and modulation-comparison analyses unless the bit-rate sweep is specifically evaluated.

Comparative performance analysis is performed to evaluate the BER, Q-factor, and SNR behavior of OOK, DPSK, and Optical OFDM in a high-capacity WDM-FSO communication system operating under atmospheric attenuation and turbulence conditions. The simulation parameters used for evaluating the proposed 8-channel WDM-FSO system are summarized in Table 2. These parameters are selected based on typical practical values used in optical wireless communication systems.

4. RESULTS

The performance of the proposed 8-channel WDM-FSO system is evaluated under fog-impaired atmospheric conditions via a comparative analysis of OOK, DPSK, and Optical OFDM modulation schemes. The investigation focuses on modulation-dependent BER, Q-factor, and SNR behaviors under atmospheric attenuation and turbulence effects.

The system operates at wavelengths ranging from 1552 nm to 1566 nm with 2 nm channel spacing. Fog-induced Mie scattering and turbulence-generated irradiance fluctuations introduce severe optical power degradation, resulting in increased BER, reduced Q-factor, and deteriorated receiver SNR. The analysis focuses on three important performance metrics: Bit Error Rate, Q-Factor, and Signal-to-Noise Ratio.

Figure 5 and Table 4 show that BER increases as the bit rate rises from 2 Gbps to 16 Gbps. This is because higher bit rates reduce bit duration, making the signal more sensitive to noise, inter-symbol interference, atmospheric fading, and EDFA noise. OOK gives the highest BER, DPSK shows better performance, and OFDM achieves the lowest BER across all bit rates.

Figure 6 and Table 5 show that BER increases as atmospheric visibility decreases from 500 m to 50 m. Lower visibility represents stronger fog or atmospheric attenuation, which reduces received optical power and degrades signal quality. OOK gives the highest BER because it is more sensitive to intensity fluctuations and noise, while DPSK provides better performance. OFDM achieves the lowest BER across all visibility values,

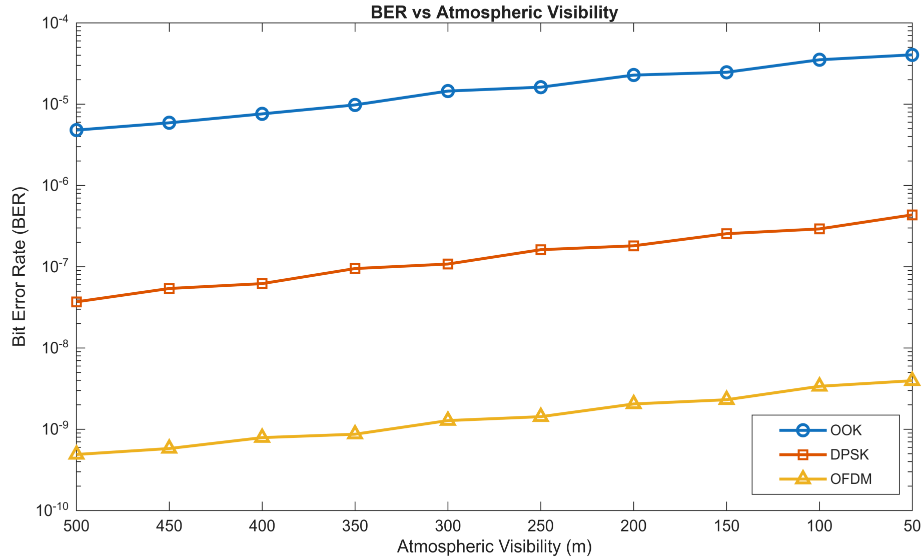

FIGURE 6. Visibility vs BER comparison.

TABLE 4. BER vs bit rate.

Bit Rate (Gbps)	Modulation	Simulated BER	Analytical BER
2	OOK	7.8×10^{-7}	7.1×10^{-7}
	DPSK	1.5×10^{-8}	1.3×10^{-8}
	OFDM	2.1×10^{-10}	1.9×10^{-10}
4	OOK	1.7×10^{-6}	1.5×10^{-6}
	DPSK	3.1×10^{-8}	2.8×10^{-8}
	OFDM	3.4×10^{-10}	3.0×10^{-10}
6	OOK	3.5×10^{-6}	3.1×10^{-6}
	DPSK	5.8×10^{-8}	5.1×10^{-8}
	OFDM	5.2×10^{-10}	4.6×10^{-10}
8	OOK	6.4×10^{-6}	5.7×10^{-6}
	DPSK	8.6×10^{-8}	7.8×10^{-8}
	OFDM	7.4×10^{-10}	6.8×10^{-10}
10	OOK	1.0×10^{-5}	9.2×10^{-6}
	DPSK	1.2×10^{-7}	1.1×10^{-7}
	OFDM	1.0×10^{-9}	9.0×10^{-10}
12	OOK	1.5×10^{-5}	1.3×10^{-5}
	DPSK	1.7×10^{-7}	1.5×10^{-7}
	OFDM	1.3×10^{-9}	1.2×10^{-9}
14	OOK	2.1×10^{-5}	1.9×10^{-5}
	DPSK	2.3×10^{-7}	2.0×10^{-7}
	OFDM	1.8×10^{-9}	1.6×10^{-9}
16	OOK	2.9×10^{-5}	2.5×10^{-5}
	DPSK	3.0×10^{-7}	2.7×10^{-7}
	OFDM	2.4×10^{-9}	2.1×10^{-9}

showing its higher robustness against atmospheric impairments in the WDM-FSO system.

Figure 7 and Table 6 show that the BER increases nonlinearly as the FSO link distance increases from 1 km to 8 km. This degradation occurs because longer propagation distance introduces higher atmospheric attenuation, beam spreading loss, turbulence effects, and EDFA amplified spontaneous emission noise, which reduce the received signal quality. OOK shows the highest BER and reaches close to the FEC limit at 8 km, indicating greater sensitivity to distance-related impairments.

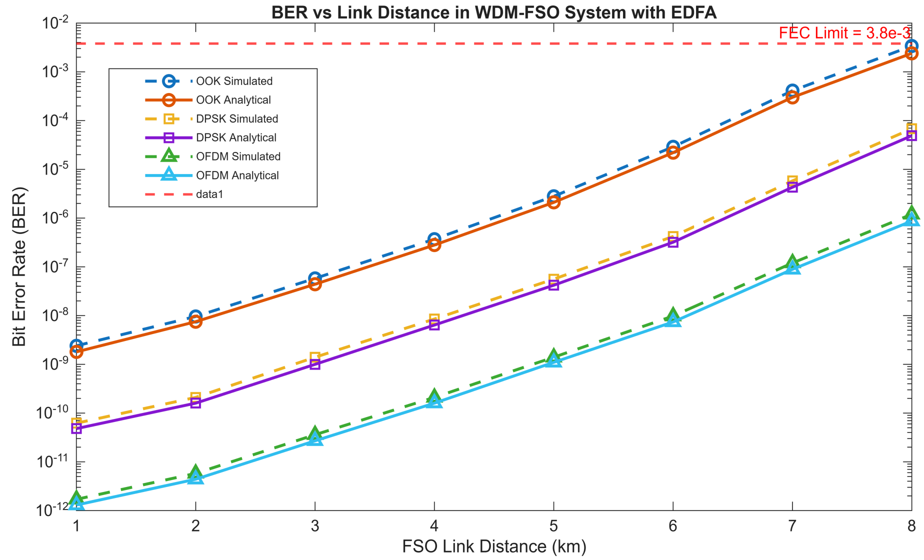

FIGURE 7. BER vs distance.

TABLE 5. Visibility vs BER under fog conditions.

Visibility (m)	OOK BER	DPSK BER	OFDM BER
500	4.8×10^{-6}	3.7×10^{-8}	4.9×10^{-10}
450	5.9×10^{-6}	5.4×10^{-8}	5.8×10^{-10}
400	7.6×10^{-6}	6.2×10^{-8}	7.9×10^{-10}
350	9.8×10^{-6}	9.5×10^{-8}	8.7×10^{-10}
300	1.45×10^{-5}	1.08×10^{-7}	1.28×10^{-9}
250	1.62×10^{-5}	1.62×10^{-7}	1.43×10^{-9}
200	2.28×10^{-5}	1.81×10^{-7}	2.05×10^{-9}
150	2.47×10^{-5}	2.55×10^{-7}	2.31×10^{-9}
100	3.52×10^{-5}	2.92×10^{-7}	3.38×10^{-9}
50	4.05×10^{-5}	4.35×10^{-7}	3.96×10^{-9}

DPSK provides better performance than OOK, while OFDM achieves the lowest BER over the entire distance range. The simulated BER values are slightly higher than the analytical values due to practical noise and component losses included in the simulation model.

Figure 8 and Table 7 show that the Q-factor decreases as the FSO link distance increases from 1 km to 8 km. This reduction occurs due to higher atmospheric attenuation, beam spreading loss, turbulence effects, receiver noise, and EDFA amplified spontaneous emission noise at longer distances. OOK shows the lowest Q-factor and experiences the highest degradation, indicating weaker tolerance to distance-related impairments. DPSK provides better performance than OOK, while OFDM maintains the highest Q-factor over the entire distance range. The analytical Q-factor values are slightly higher than the simulated values because the simulation includes practical system losses and noise effects. Overall, under the specified simulation assumptions, OFDM maintains the highest Q-factor over the evaluated distance range.

Figure 9 and Table 8 show that the SNR decreases as the FSO link distance increases from 1 km to 8 km. This reduction is caused by increased atmospheric attenuation, geometric

TABLE 6. BER vs distance.

Distance	Modulation	Simulated BER	Analytical BER
1 km	OOK	2.4×10^{-9}	1.8×10^{-9}
	DPSK	6.2×10^{-11}	4.8×10^{-11}
	OFDM	1.7×10^{-12}	1.3×10^{-12}
2 km	OOK	9.6×10^{-9}	7.5×10^{-9}
	DPSK	2.1×10^{-10}	1.6×10^{-10}
	OFDM	5.8×10^{-12}	4.4×10^{-12}
3 km	OOK	5.8×10^{-8}	4.4×10^{-8}
	DPSK	1.4×10^{-9}	1.0×10^{-9}
	OFDM	3.6×10^{-11}	2.7×10^{-11}
4 km	OOK	3.7×10^{-7}	2.8×10^{-7}
	DPSK	8.5×10^{-9}	6.4×10^{-9}
	OFDM	2.1×10^{-10}	1.6×10^{-10}
5 km	OOK	2.8×10^{-6}	2.1×10^{-6}
	DPSK	5.6×10^{-8}	4.2×10^{-8}
	OFDM	1.4×10^{-9}	1.1×10^{-9}
6 km	OOK	2.9×10^{-5}	2.2×10^{-5}
	DPSK	4.2×10^{-7}	3.2×10^{-7}
	OFDM	9.8×10^{-9}	7.4×10^{-9}
7 km	OOK	4.1×10^{-4}	3.0×10^{-4}
	DPSK	5.8×10^{-6}	4.3×10^{-6}
	OFDM	1.2×10^{-7}	8.9×10^{-8}
8 km	OOK	3.4×10^{-3}	2.4×10^{-3}
	DPSK	6.8×10^{-5}	4.9×10^{-5}
	OFDM	1.2×10^{-6}	8.7×10^{-7}

spreading loss, turbulence-induced fading, receiver noise, and EDFA amplified spontaneous emission noise over longer propagation paths. OOK exhibits the lowest SNR and falls close to the 10 dB reference level at 8 km, indicating stronger performance degradation. DPSK provides improved SNR compared with OOK, while OFDM maintains the highest SNR throughout the distance range. The analytical SNR values are slightly

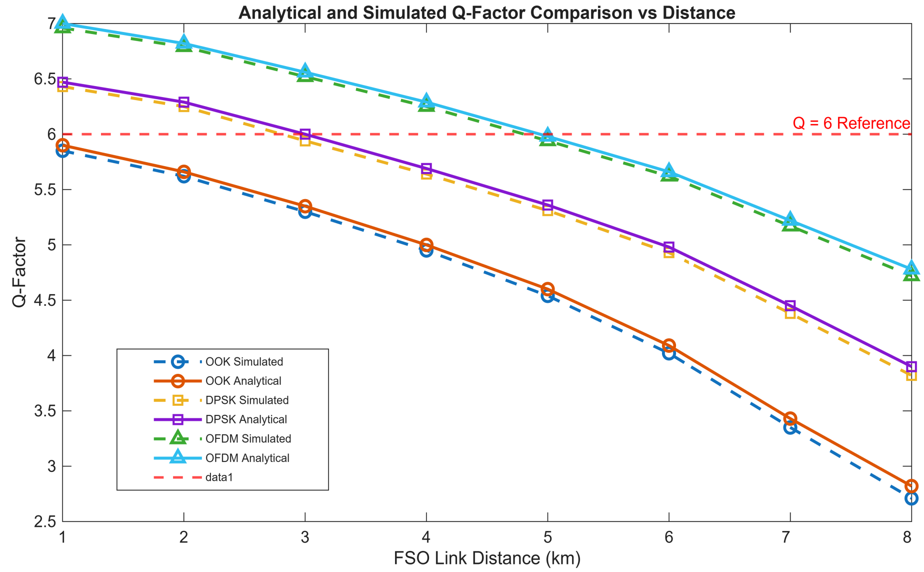

FIGURE 8. Q-factor vs distance.

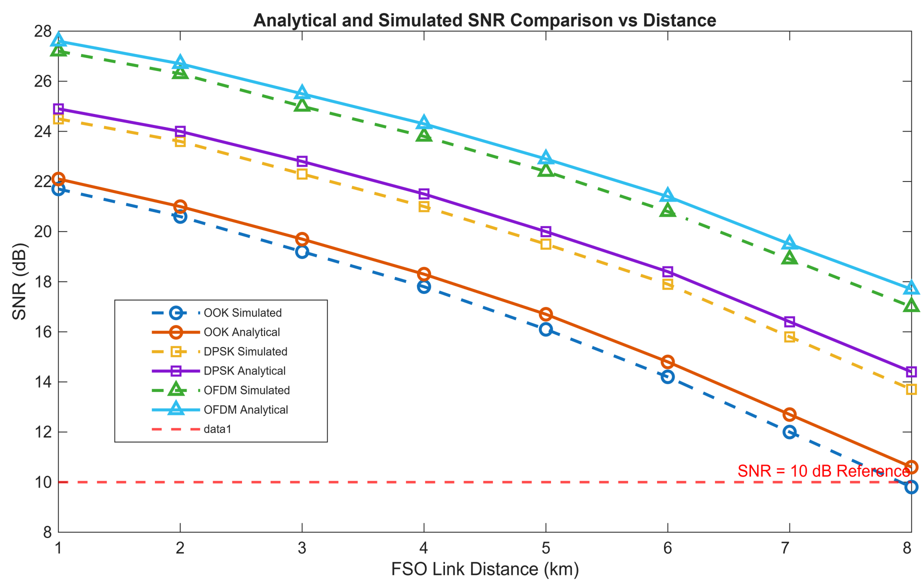

FIGURE 9. SNR vs distance.

higher than the simulated values because practical losses and noise effects are included in the simulation. Overall, under the specified simulation assumptions, OFDM maintains the highest SNR over the evaluated distance range.

4.1. Practical Impairment Sensitivity Analysis

To address practical deployment impairments, an additional sensitivity analysis is performed for the representative long-distance OFDM case at 8 km and 10 Gbps. The analysis considers beam divergence, WDM filter isolation, laser launch-power fluctuation, and receiver-side DSP-assisted normalization. The baseline condition is taken from the original 8 km OFDM result, where the simulated BER, Q-factor, and SNR are 1.2×10^{-6}, 4.72, and 17.0 dB, respectively. The sensitivity results are summarized in Table 9.

Table 9 shows that beam divergence, reduced WDM filter isolation, and laser launch-power fluctuation degrade the link by increasing BER and reducing Q-factor/SNR. The degradation is more visible at 8 km because geometric spreading and attenuation reduce the received optical power. When the beam divergence increases from 1.0 mrad to 2.0 mrad, the BER increases from 1.2×10^{-6} to 6.1×10^{-6}. With receiver-side DSP-assisted normalization and adaptive thresholding, the BER improves to 4.2×10^{-6} under the same 2.0 mrad divergence condition. Similarly, reducing WDM filter isolation to 15 dB increases interchannel leakage and degrades BER to 7.4×10^{-6}. These results confirm that practical transmitter, receiver, and WDM filtering impairments must be considered when evaluating long-distance EDFA-assisted WDM-FSO links.

TABLE 7. Q-factor vs distance.

Distance	Modulation	Simulated Q-Factor	Analytical Q-Factor
1 km	OOK	5.85	5.90
	DPSK	6.43	6.47
	OFDM	6.96	7.00
2 km	OOK	5.62	5.66
	DPSK	6.25	6.29
	OFDM	6.79	6.82
3 km	OOK	5.30	5.35
	DPSK	5.94	6.00
	OFDM	6.52	6.56
4 km	OOK	4.95	5.00
	DPSK	5.64	5.69
	OFDM	6.25	6.29
5 km	OOK	4.54	4.60
	DPSK	5.31	5.36
	OFDM	5.94	5.98
6 km	OOK	4.02	4.09
	DPSK	4.93	4.98
	OFDM	5.62	5.66
7 km	OOK	3.35	3.43
	DPSK	4.38	4.45
	OFDM	5.17	5.22
8 km	OOK	2.71	2.82
	DPSK	3.82	3.90
	OFDM	4.72	4.78

TABLE 8. SNR vs distance.

Distance	Modulation	Simulated SNR (dB)	Analytical SNR (dB)
1 km	OOK	21.7	22.1
	DPSK	24.5	24.9
	OFDM	27.2	27.6
2 km	OOK	20.6	21.0
	DPSK	23.6	24.0
	OFDM	26.3	26.7
3 km	OOK	19.2	19.7
	DPSK	22.3	22.8
	OFDM	25.0	25.5
4 km	OOK	17.8	18.3
	DPSK	21.0	21.5
	OFDM	23.8	24.3
5 km	OOK	16.1	16.7
	DPSK	19.5	20.0
	OFDM	22.4	22.9
6 km	OOK	14.2	14.8
	DPSK	17.9	18.4
	OFDM	20.8	21.4
7 km	OOK	12.0	12.7
	DPSK	15.8	16.4
	OFDM	18.9	19.5
8 km	OOK	9.8	10.6
	DPSK	13.7	14.4
	OFDM	17.0	17.7

5. DISCUSSION

The superior performance of Optical OFDM observed in the BER, Q-factor, and SNR results can be explained by its multicarrier transmission mechanism. Instead of transmitting the complete high-speed data stream on a single optical carrier waveform, OFDM divides the data into multiple orthogonal lower-rate subcarriers. This reduces the effective symbol-rate burden on each subcarrier and improves tolerance against dispersion-like distortion, turbulence-induced fading, and receiver-noise-limited degradation. The FFT-based receiver processing also helps recover the orthogonal subcarriers more effectively under the same WDM-FSO channel conditions used for OOK and DPSK. Therefore, under the specified simulation assumptions, OFDM maintains lower BER, higher Q-factor, and higher SNR, especially at longer link distances and lower visibility conditions.

However, the OFDM advantage should not be interpreted as unconditional. Optical OFDM is more sensitive to high peak-to-average power ratio, clipping distortion, laser fluctuation, phase noise, and EDFA-related nonlinear or noise enhancement effects. In WDM-FSO links, reduced demultiplexer filter isolation and channel-power imbalance can further degrade OFDM subcarrier recovery due to inter-channel leakage. The practical impairment sensitivity analysis in Table 9 therefore shows that beam divergence, reduced WDM filter isolation, including the 15 dB case below 20 dB, and laser launch-power fluctuation degrade the OFDM-based link performance. The receiver-side DSP normalization reduces decision-level mismatch, but it does not completely remove atmospheric attenuation or geometric spreading loss. Hence, the reported OFDM improvement is valid within the defined EDFA-assisted WDM-FSO simulation conditions and practical impairment assumptions.

This work distinguishes itself by integrating multi-channel WDM-FSO transmission, visibility-dependent fog attenuation, turbulence modeling, EDFA gain/noise assumptions, WDM filter-isolation sensitivity, beam-divergence modeling, laser fluctuation modeling, receiver-side DSP-assisted normalization, and modulation-dependent BER/Q-factor/SNR evaluation within a unified impairment-aware framework.

It is evident from Table 10 that existing works generally focus on limited channel configurations, individual modulation techniques, or isolated atmospheric effects. In contrast, this work provides a comparative analysis of OOK, DPSK, and Optical OFDM in an EDFA-assisted 8-channel WDM-FSO system while also considering practical impairments such as WDM filter isolation, beam divergence, laser launch-power fluctuation, and receiver-side DSP mitigation.

TABLE 9. Practical impairment sensitivity analysis for the OFDM-based WDM-FSO link at 8 km.

Impairment condition	Parameter setting	DSP	BER	Q/SNR
Baseline	$\theta = 1.0$ mrad, isolation ≥ 30 dB, no laser fluctuation	No	1.2×10^{-6}	4.72/17.0
Beam divergence	$\theta = 1.5$ mrad	No	2.8×10^{-6}	4.55/16.2
Beam divergence	$\theta = 2.0$ mrad	No	6.1×10^{-6}	4.31/15.4
Beam divergence	$\theta = 2.0$ mrad	Yes	4.2×10^{-6}	4.43/15.4
WDM filter isolation	20 dB	No	2.2×10^{-6}	4.60/16.5
WDM filter isolation	15 dB	No	7.4×10^{-6}	4.26/15.1
Laser fluctuation	$\pm 1\%$ launch-power variation	No	1.5×10^{-6}	4.67/16.8
Laser fluctuation	$\pm 3\%$ launch-power variation	No	3.6×10^{-6}	4.46/15.9

TABLE 10. Comparison between existing atmospheric impairment-aware FSO systems and proposed WDM-FSO framework.

Ref. No.	Existing FSO System / Method	Atmospheric Impairment Considered	Key Findings	Research Gap / Limitation	Difference from Proposed Work
[10]	Coherent OFDM-FSO with cascaded EDFA	Atmospheric channel loss	OFDM with EDFA improves FSO link performance and signal quality.	Focuses mainly on OFDM and EDFA, without multi-modulation comparison in an 8-channel WDM system.	Proposed work compares OOK, DPSK, and Optical OFDM in the same EDFA-assisted WDM-FSO framework.
[13]	High-speed FSO-5G using high-power EDFA	Propagation loss	High-power EDFA improves loss compensation and supports high-speed FSO-5G links.	Does not provide detailed WDM channel-based fog and turbulence analysis.	Proposed work applies EDFA in an 8-channel WDM-FSO system and evaluates BER, Q-factor, and SNR.
[3]	Atmospheric modeling of FSO transmission	Atmospheric propagation effects	Provides modeling insight for FSO transmission under atmospheric conditions.	Mainly modeling-oriented; does not compare modulation formats in WDM-FSO architecture.	Proposed work combines atmospheric modeling with practical system-level simulation and modulation comparison.
[6]	MDM-WDM FSO using DP-QPSK under real weather	Real weather conditions	Shows the importance of realistic weather modeling in FSO performance evaluation.	Does not consider EDFA-assisted 8-channel WDM-FSO with OFDM comparison.	Proposed work evaluates EDFA-assisted WDM-FSO over 1–8 km and 50–500 m visibility.
[17]	High-speed FSO for 5G data services in different Indian locations	Geographical weather variation	Shows that FSO performance changes with location and weather conditions.	Does not focus on WDM-FSO channel allocation, EDFA, and comparative modulation analysis.	Proposed work provides a unified 8-channel WDM-FSO framework for fog-impaired and turbulence-affected conditions.
Proposed Work	8-channel C-band WDM-FSO with EDFA using OOK, DPSK, and Optical OFDM	Fog attenuation, reduced visibility, turbulence, beam divergence, WDM filter isolation, and laser launch-power fluctuation	Under the specified simulation assumptions, Optical OFDM achieves the lowest BER and maintains higher Q-factor and SNR than OOK and DPSK. Additional sensitivity analysis shows that beam divergence, reduced WDM filter isolation, and laser fluctuation degrade link performance, while receiver-side DSP-assisted normalization improves decision-level stability.	Existing works generally do not jointly consider modulation comparison, EDFA practical noise contribution, WDM filter isolation, beam divergence, laser fluctuation, and DSP-assisted receiver mitigation in one WDM-FSO framework.	Integrates Kim visibility-based fog attenuation, Beer–Lambert loss, log-normal and Gamma–Gamma turbulence, EDFA gain/noise assumptions, WDM filter-isolation sensitivity, beam-divergence modeling, laser fluctuation modeling, and receiver-side DSP-assisted normalization in one framework.

6. CONCLUSION

In this work, an EDFA-assisted 8-channel WDM-FSO communication system was evaluated under fog-impaired and turbulence-affected atmospheric conditions. The proposed system integrates visibility-dependent fog attenuation using the Kim atmospheric model, Beer-Lambert propagation loss, geometric spreading due to beam divergence, and turbulence modeling using log-normal and Gamma-Gamma distributions. The performance of OOK, DPSK, and Optical OFDM modulation schemes was compared using BER, Q-factor, and SNR as the main performance metrics under the same WDM-FSO link configuration.

The results show that increasing link distance, higher bit rate, reduced visibility, beam divergence, WDM filter leakage, and laser launch-power fluctuation degrade system performance by reducing the received signal quality. Under the specified simulation assumptions, Optical OFDM provides the best BER, Q-factor, and SNR performance among the three compared modulation schemes. At 10 Gbps, Optical OFDM achieved a BER of 1.0×10^{-9}, compared with 1.2×10^{-7} for DPSK and 1.0×10^{-5} for OOK. At 8 km, Optical OFDM maintained a BER of 1.2×10^{-6}, Q-factor of 4.72, and SNR of 17.0 dB, while DPSK achieved 6.8×10^{-5} BER, 3.82 Q-factor, and 13.7 dB SNR. In contrast, OOK degraded to 3.4×10^{-3} BER, 2.71 Q-factor, and 9.8 dB SNR. Under 50 m visibility, Optical OFDM achieved the lowest BER of 3.96×10^{-9}.

The additional practical-impairment sensitivity analysis shows that beam divergence, reduced WDM filter isolation, and laser launch-power fluctuation can further degrade the OFDM-based WDM-FSO link, especially at longer distances. The receiver-side DSP-assisted normalization and adaptive thresholding method improves decision-level stability under beam-divergence-induced received-power variation, but it does not eliminate atmospheric attenuation or geometric spreading loss. Therefore, the evaluated EDFA-assisted WDM-FSO system indicates potential for high-capacity terrestrial optical wireless communication under the considered simulation conditions, while practical deployment should also consider OFDM PAPR, EDFA noise figure, WDM filter isolation, laser fluctuation, pointing stability, and outdoor experimental validation. Future work can extend the study by using adaptive EDFA gain control, coding-assisted OFDM, hybrid RF/FSO backup links, real-time weather-aware modulation selection, and experimental validation under practical atmospheric conditions.

REFERENCES

[1] Jahid, A., M. H. Alsharif, and T. J. Hall, "A contemporary survey on free space optical communication: Potentials, technical challenges, recent advances and research direction," *Journal of Network and Computer Applications*, Vol. 200, 103311, 2022.

[2] Alimi, I. A. and P. P. Monteiro, "Revolutionizing free-space optics: A survey of enabling technologies, challenges, trends, and prospects of beyond 5G free-space optical (FSO) communication systems," *Sensors*, Vol. 24, No. 24, 8036, 2024.

[3] Czerwinski, A., "Atmospheric modeling of free-space optical transmission: Satellite downlinks and horizontal channels," *Optical and Quantum Electronics*, Vol. 57, No. 10, 577, 2025.

[4] Xu, Z., G. Xu, and Z. Zheng, "BER and channel capacity performance of an FSO communication system over atmospheric turbulence with different types of noise," *Sensors*, Vol. 21, No. 10, 3454, 2021.

[5] Belgaonkar, V. V., R. Sundaraguru, and C. Poongothai, "Enhancing free space optical system performance through fog and atmospheric turbulence using power optimization," *Engineering, Technology & Applied Science Research*, Vol. 15, No. 1, 19 390–19 395, 2025.

[6] Kaur, T., S. Kaur, and M. Ijaz, "Modeling and performance analysis of MDM−WDM FSO link using DP-QPSK modulation under real weather conditions," *Telecom*, Vol. 6, No. 2, 29, 2025.

[7] Periyasamy, K., V. Rathinam, K. Ganesan, M. Ramachandran, S. Muthusamy, R. Lamba, H. Panchal, M. Shanmugam, S. P. S. N. Jalajakumari, and R. Kottapalli, "A novel method for analyzing the performance of free space optical communication in WDM using EDFA," *Wireless Personal Communications*, Vol. 131, No. 1, 679–707, 2023.

[8] Yaseen, M. A., A. K. Abass, and S. M. Abdulsatar, "Improving of wavelength division multiplexing based on free space optical communication via power comparative system," *Wireless Personal Communications*, Vol. 119, No. 1, 381–391, 2021.

[9] El-Nahal, F., T. Xu, D. AlQahtani, and M. Leeson, "A bidirectional wavelength division multiplexed (WDM) free space optical communication (FSO) system for deployment in data center networks (DCNs)," *Sensors*, Vol. 22, No. 24, 9703, 2022.

[10] Kumar, S. and Payal, "Enhancing performance of coherent optical OFDM FSO communication link using cascaded EDFA," *Wireless Personal Communications*, Vol. 120, No. 2, 1109–1123, 2021.

[11] Anandkumar, D. and R. G. Sangeetha, "A survey on performance enhancement in free space optical communication system through channel models and modulation techniques," *Optical and Quantum Electronics*, Vol. 53, No. 1, 5, 2021.

[12] Shi, Y., A. Armghan, F. Ali, K. Aliqab, and M. Alsharari, "Enriching capacity and transmission of hybrid WDM-FSO link for 5G mobility," *Photonics*, Vol. 10, No. 2, 121, 2023.

[13] Hayle, S. T., H.-Y. Hsu, C.-P. Wang, H.-H. Lu, J.-M. Lu, W.-W. Hsu, Y.-C. Chung, Y.-Y. Bai, and K. Okram, "High-speed FSO-5G wireless communication system with enhanced loss compensation using high-power EDFA," *Scientific Reports*, Vol. 15, No. 1, 379, Jan. 2025.

[14] Ajewole, B. D., K. O. Odeyemi, P. A. Owolawi, and V. M. Srivastava, "Performance of OFDM-FSO communication system with different modulation schemes over gamma-gamma turbulence channel," *Journal of Communications*, Vol. 14, No. 6, 490–497, 2019.

[15] Sangeetha, R. G., C. Hemanth, and I. Jaiswal, "Performance of different modulation scheme in free space optical transmission — A review," *Optik*, Vol. 254, 168675, Mar. 2022.

[16] Singh, M. and J. Malhotra, "Performance comparison of M-QAM and DQPSK modulation schemes in a 2 × 20 Gbit/s-40 GHz hybrid MDM-OFDM-based radio over FSO transmission system," *Photonic Network Communications*, Vol. 38, No. 3, 378–389, 2019.

[17] Singh, H., N. Mittal, R. Miglani, H. Singh, G. S. Gaba, and M. Hedabou, "Design and analysis of high-speed free space optical (FSO) communication system for supporting fifth generation (5G) data services in diverse geographical locations of India," *IEEE Photonics Journal*, Vol. 13, No. 5, 1–12, Oct. 2021.

[18] Sharma, A., S. Kaur, and S. Chaudhary, "Performance analysis of 320 Gbps DWDM—FSO system under the effect of different atmospheric conditions," *Optical and Quantum Electronics*,

Vol. 53, No. 5, 239, 2021.

[19] Obaid, H. M., Z. B. Javaid, T. Mazhar, M. A. Nadeem, M. M. Saeed, and H. Hamam, "Performance analysis of a 400-Gbps DWDM-FSO system using advanced modulation formats and under adverse weather conditions," *Discover Sustainability*, Vol. 5, No. 1, 301, 2024.

[20] Kaur, S., R. Goyal, S. Chaudhary, *et al.*, "1000 Gbps MDM-WDM FSO link employing DP-QPSK modulation scheme under the effect of fog," *Optik*, Vol. 257, 168809, May 2022.

[21] Morichetti, F., G. Cavicchioli, A. Martinez, S. Seyedinnavadeh, F. Zanetto, C. Mazzucco, *et al.*, "Mitigation of atmospheric turbulence in an optical free space link with an integrated photonic processor," in *2023 Optical Fiber Communications Conference and Exhibition (OFC)*, San Diego, CA, USA, 2023.

[22] Srivastava, V., A. Mandloi, and G. G. Soni, "Outage probability and average BER estimation of FSO system employing wavelength diversity," *Optical and Quantum Electronics*, Vol. 51, 229, 2019.

[23] Mukherjee, R., K. Mallick, B. Kuiri, S. Santra, B. Dutta, P. Mandal, and A. S. Patra, "PAM-4 based long-range free-space-optics communication system with self injection locked QD-LD and RS codec," *Optics Communications*, Vol. 476, 126304, Dec. 2020.

[24] Ali, M. A. A., F. K. Shaker, and H. A. Kadhum, "Investigation and analysis of data rate for free space optical communications system under dust conditions," *Wireless Personal Communications*, Vol. 113, No. 4, 2327–2338, 2020.

[25] Kumar, L. B. and P. Krishnan, "Multi-hop convergent FSO-UWOC system to establish a reliable communication link between the islands," *Optics Communications*, Vol. 474, 126107, Nov. 2020.

[26] Kumar, A. and P. Krishnan, "Performance analysis of RoFSO links with spatial diversity over combined channel model for 5G in smart city applications," *Optics Communications*, Vol. 466, 125600, Jul. 2020.

[27] Kumar, A. and P. Krishnan, "Performance analysis of radio-over-free-space optical communication system with spatial diversity over combined channel model," *Optical and Quantum Electronics*, Vol. 54, No. 4, 211, 2022.

[28] Singh, M., A. Atieh, and D. Kakati, "200 Gbps free-space optics data transmission using orbital angular momentum multiplexed beams and PAM-4 signals," *Optical and Quantum Electronics*, Vol. 55, No. 1, 24, 2023.

[29] Dutta, B., B. Kuiri, S. Santra, N. Sarkar, I. A. Biswas, R. Atta, and A. S. Patra, "100 Gbps data transmission based on different l-valued OAM beam multiplexing employing WDM techniques and free space optics," *Optical and Quantum Electronics*, Vol. 53, No. 9, 515, 2021.

[30] Singh, M., A. Atieh, A. Grover, and O. Barukab, "Performance analysis of 40 Gb/s free space optics transmission based on orbital angular momentum multiplexed beams," *Alexandria Engineering Journal*, Vol. 61, No. 7, 5203–5212, 2022.

[31] Singh, M. and J. Malhotra, "Performance comparison of different modulation schemes in high-speed MDM based radio over FSO transmission link under the effect of atmospheric turbulence using aperture averaging," *Wireless Personal Communications*, Vol. 111, No. 2, 825–842, 2020.

[32] EL-Qady, A. and M. Abaza, "Performance analysis of the effects of atmospheric turbulence on free space optical communication using multi-hop decode and forward relay in north and south of Egypt," *Optical and Quantum Electronics*, Vol. 56, No. 8, 1373, 2024.

[33] Qu, C., S. Ghafoor, A. Ahmad, J. Mirza, A. J. Aljohani, and I. Aziz, "A bidirectional free space optical link for last-mile terrestrial access links employing a novel wavelength shift keying technique," *Optical and Quantum Electronics*, Vol. 56, No. 8, 1367, 2024.

[34] Singh, M., A. Atieh, M. H. Aly, and S. A. A. El-Mottaleb, "A PAM-4 signal enabled 400 Gbps hybrid PDM-OAM multiplexing-based FSO transmission system," *Optical and Quantum Electronics*, Vol. 56, No. 7, 1259, 2024.

[35] Wen, Y., F. Yang, J. Song, and Z. Han, "Free-space optical integrated sensing and communication based on DCO-OFDM: Performance metrics and resource allocation," *IEEE Internet of Things Journal*, Vol. 12, No. 2, 2158–2173, Jan. 2025.

[36] Aljohani, A. J., J. Mirza, and S. Ghafoor, "A novel regeneration technique for free space optical communication systems," *IEEE Communications Letters*, Vol. 25, No. 1, 196–199, Jan. 2021.

[37] Bekkali, A., H. Fujita, and M. Hattori, "New generation free-space optical communication systems with advanced optical beam stabilizer," *Journal of Lightwave Technology*, Vol. 40, No. 5, 1509–1518, 2022.